Resonant Mode Transition in the RF-Controlled Hollow Cathode

IEPC-2013-205

Presented at the 33rd International Electric Propulsion Conference,
The George Washington University, Washington, D.C., USA
October 6–10, 2013

Matthew L. Plasek,* Christopher J. Wordingham, † Edgar Y. Choueiri ‡
Princeton University, Princeton, NJ, 08544, USA

The mechanism behind a sharp transition from low- to high-plasma-density modes that was recently discovered through numerical simulations of a promising hollow cathode concept is investigated using numerical modeling. The RF-Controlled Hollow Cathode concept adds radio-frequency power to a large-diameter cathode for high-power, long-lifetime electric thruster applications. By exploring the basic parameters and behavior of a simplified two-dimensional model where an RF plasma is introduced into a thermionic cathode, it was found that a nonlinear transition was caused by both a jump in the electric field amplitude due to a resonant cavity condition and an increase in the reduced electric field E/n_0 from neutral depletion. This transition results in an increase of the maximum plasma density by an order of magnitude, which benefits the cathode's operational lifetime and discharge current capability. Surface waves were ruled out as a transition contributor as the model does not account for them, though they may be present in future experimental studies. Evidence for a beneficial hysteresis in the operational parameters of the cathode is also presented.

Nomenclature

c = speed of light in vacuum
E = electric field
k = wavenumber
n_0 = neutral gas number density
n_e = electron number density
n_c = cutoff plasma density
n_{sw} = surface wave plasma density criterion
P_{in} = input RF power
P_r = reflected RF power
Γ = reflection coefficient
δ = skin depth
ϵ = relative permittivity
λ = wavelength
ω_p = electron plasma frequency
ω = incident RF frequency

*Graduate Research Assistant, EPPDyL; Mechanical and Aerospace Engineering Dept., mplasek@princeton.edu.
†Graduate Research Assistant, EPPDyL; Mechanical and Aerospace Engineering Dept., cjw4@princeton.edu.
‡Chief Scientist, EPPDyL; Professor, Applied Physics, Mechanical and Aerospace Engineering, choueiri@princeton.edu.

I. Introduction

STATE-of-the-art hollow cathodes used in ion and Hall thrusters have met most solar electric propulsion and commercial satellite lifetime requirements through extended operational life tests approaching 50,000 hours (50 kh).[1,2] However, previously proposed nuclear electric propulsion missions[3] to interplanetary destinations require lifetimes up to 100 kh. In addition to extended lifetimes, power levels available for propulsion are expected to increase by an order of magnitude in the next few decades as extrapolated from recent trends in space power generation. The U.S. Air Force Research Laboratory (AFRL) projects that next-generation electric thrusters will need to be capable of processing 100-200 kW of power, dwarfing the 0.5 to 12 kW range of recent focus.[4] At the specific impulse levels relevant to Air Force missions (between 2000-6000 seconds), this translates to roughly 330-660 A of discharge current – one order of magnitude higher than currents commonly used in electric thrusters today, e.g., the nominal 20 A for a 6 kW laboratory Hall thruster.[5] In order to take advantage of higher power levels, a 50 kW-class Hall thruster has been developed at NASA.[6] This Hall thruster was recently tested up to 100 A of discharge current, exemplifying the need for higher performance cathodes explicitly designed to handle high discharge currents while providing extended operational life.

Recent progress made by Goebel and Chu[7] includes testing a lanathanum hexaboride (LaB_6) bulk-emitting hollow cathode that can produce up to 300 A of discharge current while maintaining an expected life of 10-20 kh. Van Noord, et al.[8] describe the design and testing of a dispenser cathode at 50 A with a predicted life of 100 kh. Even with these selected advances, the scale of needed improvement in the next few decades warrants the pursuit of novel cathode concepts that can meet both requirements of 100 kh of operational lifetime and greater than a 600 A maximum discharge current.

In the internal cavity of hollow cathodes, a sharp peak in plasma density corresponds to a small current "attachment" area, or plasma-emitter contact area. This restricted current attachment area leads to high current densities and high temperatures within a limited axial depth inside the cathode as reported previously.[9–11] Farther upstream from this dense plasma region, the plasma density is too low to support significant thermionic emission and the low-work-function emitter is space charge limited,[5] as shown schematically in Fig. 1. Taking advantage of the full axial length of the emitter for electron emission requires that the axial profiles of plasma density and emitter temperature be "flatter" and more uniform along the entire emitter length.

The operational life of a hollow cathode can be estimated to first order based on the evaporation rate of the emitter material which varies with the current density.[12] Therefore, by maintaining the same discharge current while increasing the current attachment area, we expect the resulting lower peak in the axial profiles of both current density and emitter temperature to correspond to increased cathode lifetime.[5] Meeting this goal allows the operator to choose some optimal balance between increasing the operational lifetime and increasing the discharge current to desired levels.

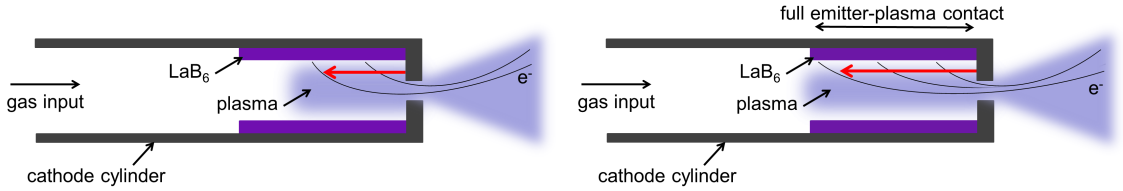

Figure 1. Cutaway side views of a basic hollow cathode schematic showing the typical limited current attachment area along the length of the LaB_6 emitter (left) compared to the goal of current attachment to the full emitter area (right).

We are constructing a proof-of-concept experiment for the novel RF-Controlled Hollow Cathode (RF-CHC) concept that motivates this analysis and past modeling.[13,14] Our results in this paper will be used to inform the future acquisition and interpretation of experimental data and to gain physical insight. The goal of these efforts is to address the simple question: What are the effects of adding RF or microwave energy to a thermionic hollow cathode? In the context of the literature, one might consider the RF-Controlled Hollow Cathode concept to be a unification of thermionic hollow cathodes[10,11] and microwave plasma electron sources.[15] This unifying design has the potential to be attractive for high-power, long-lifetime electric propulsion applications.

Our initial modeling[13,14] examined the concept of controlling current attachment along the length of the cathode's major axis by adding radio frequency (RF) energy to the upstream end of a hollow cathode. This concept of the RF-Controlled Hollow Cathode relies on generating an overdense plasma upstream that is comparable in density to the typical cathode plasma adjacent to the orifice. From modeling the RF-CHC,[14] we found that a direct coaxial-cathode mating configuration can lead to high percentages (>96%) of localized RF power absorption when the RF inner coaxial conductor was positioned at an appropriate axial distance from the orifice. The RF inner coaxial conductor extending into the hollow cathode acted as a stinger, as approximately 62% of the RF power was absorbed within 2 mm of the inner coaxial conductor tip.

We also simulated the effects of RF power input in another configuration of the RF-CHC[13] in which a waveguide is mated directly to the upstream end of the cathode, hence treating the hollow cathode as a waveguide or a resonant cavity. This two-dimensional numerical modeling[13] led to the discovery of a sharp, order-of-magnitude transition in the maximum plasma density showing strong RF power and pressure dependence.

We investigate this pronounced transition or "jump" through analysis of our numerical modeling starting with a brief description of the RF-CHC in Section II. We continue with an analysis and discussion of the transition's cause and describe new evidence of hysteresis behavior in Section III.

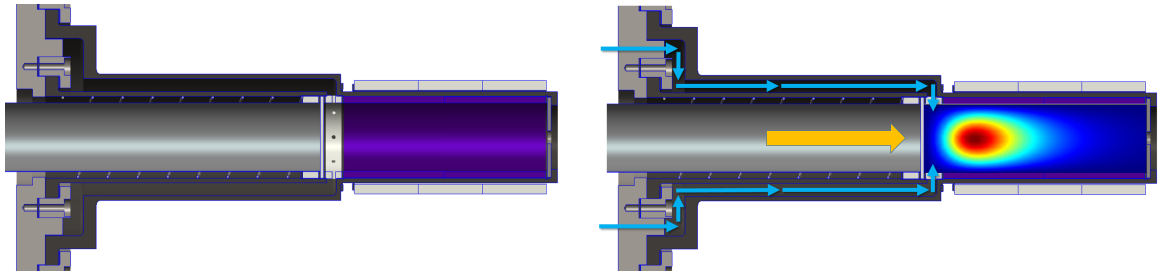

Figure 2. Side cutaway views of the RF-CHC waveguide configuration. The orange arrow depicts microwave propagation, light blue arrows depict the neutral gas injection path, and the downstream emitter region on the right shows an example plasma density simulation result, matching the bounds of our cathode cavity model. The purple region in the left image is the LaB_6 insert.

II. Description of the RF-Controlled Hollow Cathode

The goal of the RF-Controlled Hollow Cathode (RF-CHC) as a high-power, high-current-density cathode is to control or maximize the axial extent of significant current attachment to the electron-emitting insert. In order to support emitter current densities of greater than 20 A/cm^2 common for bulk-emitting LaB_6 emitters,[10] plasma densities greater than 2×10^{19} m^{-3} must exist upstream. The strategy of the RF-CHC is to augment the typical downstream thermionic plasma with an upstream microwave plasma of comparable density in order to create a more uniform axial profile of the plasma density. Details of our numerical modeling and of the present configuration can be found in Ref. 13.

The analyzed configuration, as shown in Fig. 2, adds RF power via a waveguide at what are more typically known in the literature as microwave frequencies (GHz). However, in the interest of unambiguous continuity and relying on the broad definition of radio frequency, we refer to this configuration as an RF-Controlled Hollow Cathode and use "microwave" and "RF" interchangeably though we refer to the same incident frequency. The added RF power creates an overdense plasma that is dependent on the incident frequency[16] and is comparable in density to large-diameter cathode plasmas.[13,15] Twice the inner diameter of other high-power cathodes studied,[7] the RF-CHC is itself a large-diameter cathode (inner diameter = 2.7 cm) which impacts thermal heating and losses, internal neutral gas pressure, and the waveguide cutoff frequency. Considering reasonable cathode dimensions, the benefits of a larger diameter on cathode behavior,[7,17] and the desired plasma density, a design frequency of 8 GHz was selected.

III. Analysis and Discussion

A. Resonant Cavity Mode Transition

As presented in Fig. 3, we recently observed through numerical simulations[13] the occurrence of a sharp transition in emitted thermionic current over a range of incident RF powers. The transition also corresponds to jumps in plasma density, local electron temperature, and plasma potential depending on both the internal neutral gas pressure and incident RF power. This transition was attributed[13] to the onset of a cavity resonance condition which resulted in the incident electric field increasing dramatically as shown in Fig. 4. The dependence on incident power and pressure can be explained by noting that these two parameters affect the axial location of the critical plasma density at which the incident microwaves are reflected. The shifting and expanding of the critical plasma density (Fig. 5) becomes a "self-tuning" mechanism in which the plasma acts as a lossy conductive resonator wall that tunes the cavity. At a minimum pressure and RF power, this tuning that results from the spatially shifting critical plasma density creates a microwave cavity resonance.

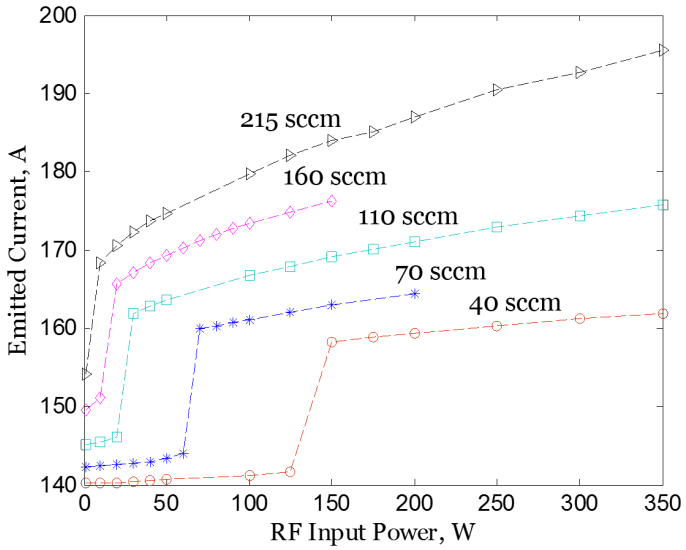

Figure 3. Emitted current versus RF power for five different flow rates corresponding to pressures used in our simulations. Note the sharp transition in emitted (thermionic) current and the transition's dependence on RF power and gas flow rate. Average cathode plasma densities mirror these trends.

In the literature, one finds similar phenomena to those uncovered in our modeling such as spatial shifts in plasma density,[18,19] abrupt increases in plasma density,[19,20] and overdense microwave-generated plasmas with power absorption taking place over a small skin depth.[15,18,21] Others have shown that these behaviors can result from "surface waves" or microwave fields propagating along a dielectric-plasma boundary in thin tubes and in large-area plasma sources.[21]

Similar to surface wave behavior, our modeled plasma varies rapidly along the cathode's major axis near the microwave window. Electron temperature spikes near the window from heating due to the incident RF waves, although only by a few tenths of eV over the insert-plasma averaged electron temperature around 1.2 eV. We also observe an inhomogenous plasma that is sharply increasing in density downstream from the window boundary. After the transition, our plasma typically meets the plasma density criterion for surface waves $n_{sw} = n_c(1+\epsilon)$,[21] where n_c is the cutoff plasma density corresponding to a plasma frequency equal to the incident RF frequency ($\omega_p = \omega$). In the RF-CHC, using a boron nitride window, the surface wave criterion density is 4.0×10^{18} m^{-3}. Although there is evidence that surface waves may contribute to a sharp transition under experimental conditions, we have ruled out surface waves as causing the observed transition as our two-dimensional numerical model (using COMSOL v4.3) does not account for fields propagating normal to the cathode major axis. We expect RF-CHC behavior may vary in experimental testing from our numerical modeling due to the potential for surface waves to be present.

Next in our analysis of the transition, we consider the location of the critical plasma density that reflects the incident microwaves. For 8 GHz this critical density is about 8×10^{17} m^{-3}. Figure 5 shows an expanding

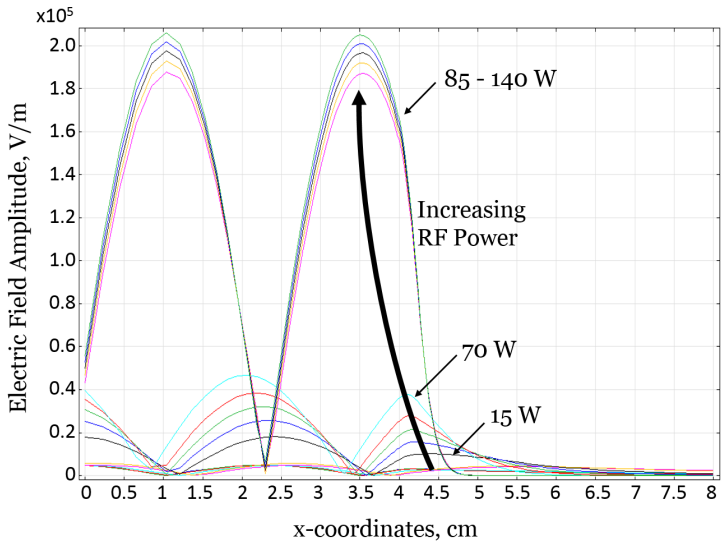

Figure 4. RF electric field amplitude curves for different RF powers as a function of waveguide position. At a critical RF power the electric field amplitude jumps in magnitude due to a cavity resonance condition. Note that the structure of the electric field amplitude changes significantly after the jump.

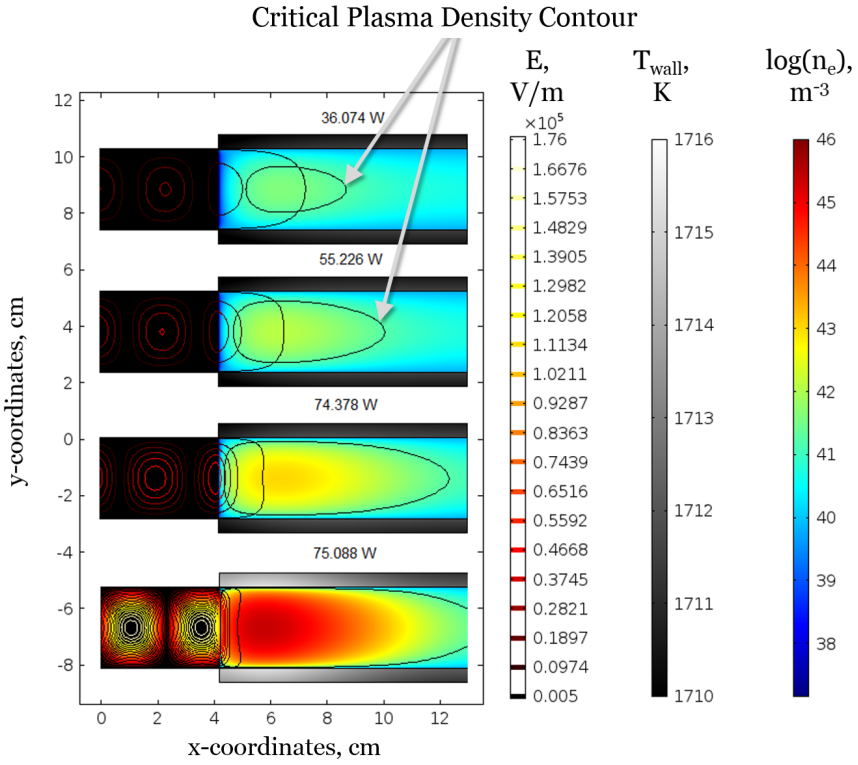

Figure 5. Progression of the critical electron density (8×10^{17} m^{-3}) contour with increasing RF power, showing the transition occurring as the critical density reaches the upstream window.

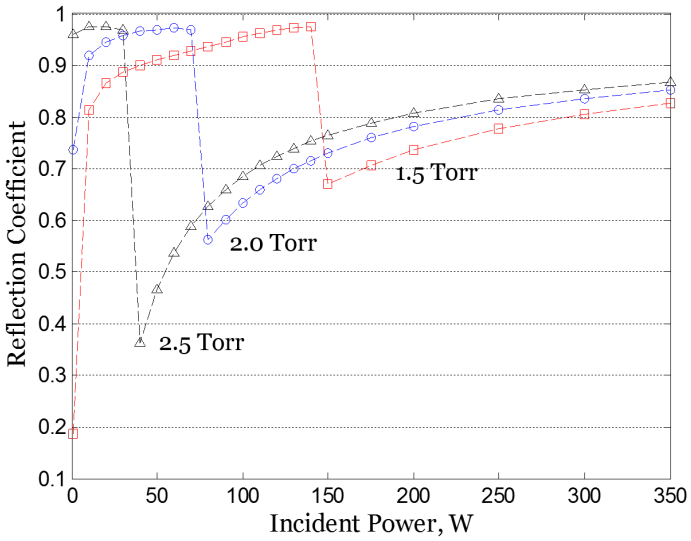

Figure 6. The reflection coefficient as a function of input RF power and pressure. Note the larger dip at the transition for higher pressures, corresponding to more efficient power absorption. At low RF powers and low pressure (1.5 Torr), the plasma density is below the critical density for RF reflection.

plasma density contour of 8×10^{17} m^{-3} with increasing incident power. We can see that the countour expands to nearly the entire insert region and contacts the microwave window at the upstream end as the transition occurs. This corresponds to the RF power being reflected near the window-plasma boundary and RF power absorption taking place mostly within a skin depth ($\sim c/\omega_p$), which is a few millimeters from the window in our case.

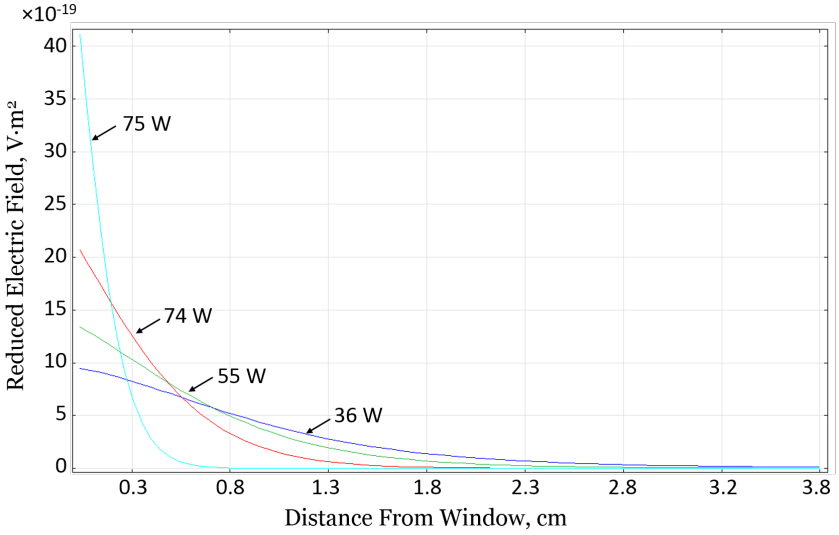

Figure 7. The reduced electric field amplitude E/n_0 for different input RF powers, with these four cases matching those in Fig. 5. The reduced electric field increases with RF power as the skin depth decreases.

In Fig. 6 we see significant, sharp dips in the reflection coefficient Γ where $\Gamma = P_r/P_{in}$. For higher pressures these drops in Γ occur at lower incident RF powers and are more extreme. This behavior of the reflection coefficient at the transition points to a nonlinearly increasing reduced electric field, defined as E/n_0, corresponding to efficient RF power absorption.[22] Due to the resonant cavity effects at the transition, the electric field amplitude jumps as seen in Fig. 4. In addition, as more power is absorbed, the neutral gas density decreases due to ionization near the window, causing a more pronounced increase in the reduced

electric field (as seen in Fig. 7) leading to a local spike in electron temperature.[22] This, in turn, increases the plamsa potential and causes increased heating of the emitter from enhanced electron and ion fluxes to the wall. The higher-temperature emitter emits increased electron current and the effect cascades through the cathode. It is this physical mechanism of the nonlinearly increased reduced electric field, in addition to the resonant cavity mode, that causes the abrupt transition we observed in our numerical modeling.

We also note in Fig. 6 that dips in the reflection coefficient at low RF powers (< 20 W) occur because at lower pressures (e.g., 1.5 Torr), the plasma is not dense enough to reflect a majority of the incident RF, i.e., $\omega_p < \omega$. For higher RF powers after the transition, the plasma density increases, the skin depth decreases, and higher reflection results.

B. Hysteresis

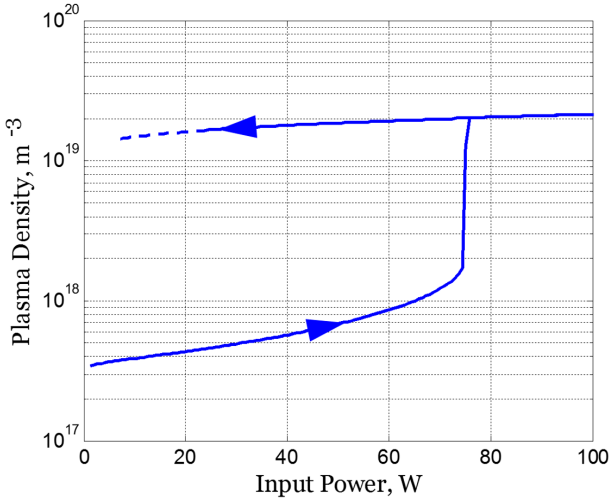

Figure 8. The average electron number density over the simulated emitter area is shown as a function of input RF power as the RF power is increased from 0 to 100 W and then slowly reduced to 0 W. The jump behavior as the input power is increased and the hysteresis in the plasma density as the power is decreased are both evident. The low RF power range (< 20 W) of the upper branch may not have reached a steady-state solution.

Microwave plasma sources have been shown to exhibit hysteresis,[21] or plasma behavior dependent on a "memory" of its operational past. This means that the plasma can have multiple operating modes even at the same operating parameters depending on the source's recent operating history. In the case of the RF-CHC, we also found evidence of strong hysteresis, as shown in Fig. 8. The hystersis in Fig. 8 is expected to be fairly accurate due to the slow change in RF power in our numerical simulation. However, for lower RF powers we may anticipate some discrepancy with future experimental measurements as the simulation may not have reached steady state. Any significant amount of hysteresis in RF-CHC operation will decrease the power budget requirement for increased lifetime and high-current operation.

IV. Conclusion

We have shown that the increase in the electric field amplitude due to cavity resonance is not the only cause of the numerically observed jump in emitted current and plasma density. The greater absorption of RF power, driven by the reduced electric field, also contributes significantly to the transition, allowing the addition of RF power to a thermionic cathode to achieve order-of-magnitude jumps in plasma density. Numerically-modeled evidence informed by the literature supports our physical interpretation of the transition and points toward significant hysteresis effects. Although not represented in our model, surface waves may be present and affect the mode-transition behavior in our upcoming experiments.

Acknowledgments

This research has been supported by the U.S. Air Force Office of Scientific Research.

References

[1]Shastry, R., Herman, D. A., Soulas, G. C., and Patterson, M. J., "NASAs Evolutionary Xenon Thruster (NEXT) Long-Duration Test as of 736 kg of Propellant Throughput," 48th AIAA Joint Propulsion Conference, Atlanta, Georgia, 2012, pp. 1–20.

[2]Shastry, R., "Status of NASAs Evolutionary Xenon Thruster (NEXT) Long-Duration Test as of 50,000 h and 900 kg Throughput," 33rd International Electric Propulsion Conference, No. IEPC-2013-121 (unpublished), Washington, D.C., 2013.

[3]Hofer, R. R., Randolph, T. M., Oh, D. Y., Snyder, J. S., and de Grys, K. H., "Evaluation of a 4.5 kW Commercial Hall Thruster System for NASA Science Missions," 42nd Joint Propulsion Conference, Sacramento, California, 2006.

[4]Brown, D. L., Beal, B. E., and Haas, J. M., "Air Force Research Laboratory High Power Electric Propulsion Technology Development," IEEEAC, 2009.

[5]Goebel, D. M., Jameson, K. K., and Hofer, R. R., "Hall Thruster Cathode Flow Impact on Coupling Voltage and Cathode Life," Journal of Propulsion and Power, Vol. 28, No. 2, March 2012, pp. 355–363.

[6]Soulas, G. C., Haag, T. W., Herman, D. A., Huang, W., Kamhawi, H., and Shastry, R., "Performance Test Results of the NASA-457M v2 Hall Thruster," 48th AIAA Joint Propulsion Conference, Atlanta, Georgia, 2012, pp. 1–17.

[7]Goebel, D. M. and Chu, E., "High Current Lanthanum Hexaboride Hollow Cathode 20-to-100 kW Class Hall Thrusters," 48th AIAA Joint Propulsion Conference, Atlanta, Georgia, 2012, pp. 1–11.

[8]Van Noord, J. L., Kamhawi, H., and Mcewen, H. K., "Characterization of a High Current, Long Life Hollow Cathode," 29th International Electric Propulsion Conference, Princeton, New Jersey, 2005, pp. 1–12.

[9]Katz, I., Mikellides, I. G., Goebel, D. M., and Polk, J. E., "Insert Heating and Ignition in Inert-Gas Hollow Cathodes," IEEE Transactions on Plasma Science, Vol. 36, No. 5, 2008, pp. 2199–2206.

[10]Goebel, D. M. and Katz, I., Fundamentals of Electric Propulsion: Ion and Hall Thrusters, Vol. 1, John Wiley & Sons Inc, 2008.

[11]Polk, J. E., Mikellides, I. G., Katz, I., and Capece, A. M., "Tungsten and Barium Transport in the Internal Plasma of Hollow Cathodes," Journal of Applied Physics, Vol. 105, No. 11, 2009, pp. 113301.

[12]Sarver-Verhey, T. R., "Scenario for Hollow Cathode End-of-Life," 26th International Electric Propulsion Conference, Kitakyushu, Japan, 1999, pp. 703–713.

[13]Plasek, M. L., Wordingham, C. J., and Choueiri, E. Y., "Modeling and Development of the RF-Controlled Hollow Cathode Concept," 49th Joint Propulsion Conference, San Jose, CA, 2013.

[14]Plasek, M. L., Jorns, B., Choueiri, E. Y., and Polk, J. E., "Exploration of RF-Controlled High Current Density Hollow Cathode Concepts," 48th AIAA Joint Propulsion Conference, Atlanta, Georgia, 2012, pp. 1–17.

[15]Diamant, K. D., "Resonant Cavity Plasma Electron Source," IEEE Transactions on Plasma Science, Vol. 37, No. 8, Aug. 2009, pp. 1558–1562.

[16]Foster, J. E. and Patterson, M. J., "Characterization of 40-Centimeter Microwave Electron Cyclotron Resonance Ion Source and Neutralizer," Journal of Propulsion and Power, Vol. 21, No. 5, 2005, pp. 1–5.

[17]Salhi, A. and Turchi, P. J., "Scaling Relations for Design and Operation of Orificed-Hollow Cathodes," 30th Joint Propulsion Conference, Indianapolis, Indiana, 1994, pp. 0–7.

[18]Zhu, Y., Modeling of a Microwave Plasma Electron Source for Neutralization of Ion Thrusters, Ph.D. thesis, University of Toulouse, 2013.

[19]Sugai, H., Ghanashev, I., and Nagatsu, M., "High-Density Flat Plasma Production Based on Surface Waves," Plasma Sources Science and Technology, Vol. 7, No. 2, 1998, pp. 192–205.

[20]Sugai, H., Ghanashev, I., and Mizuno, K., "Transition of electron heating mode in a planar microwave discharge at low pressures," Applied Physics Letters, Vol. 77, No. 22, 2000, pp. 3523.

[21]Ganachev, I. P. and Sugai, H., "Production and control of planar microwave plasmas for materials processing," Plasma Sources Science and Technology, Vol. 11, 2002, pp. A178–A190.

[22]Hagelaar, G. J. M., Hassouni, K., and Gicquel, A., "Interaction between the electromagnetic fields and the plasma in a microwave plasma reactor," Journal of Applied Physics, Vol. 96, 2004, pp. 1819.